isvr Institute of Sound and Vibration Research

Stability and Accuracy of Finite Element Methods for Flow Acoustics: 1. One Dimensional Acoustic Propagation

G.Gabard and R.J. Astley

ISVR Technical Report No 301

September 2003

University of Southampton

SCIENTIFIC PUBLICATIONS BY THE ISVR

Technical Reports are published to promote timely dissemination of research results by ISVR personnel. This medium permits more detailed presentation than is usually acceptable for scientific journals. Responsibility for both the content and any opinions expressed rests entirely with the author(s).

Technical Memoranda are produced to enable the early or preliminary release of information by ISVR personnel where such release is deemed to the appropriate. Information contained in these memoranda may be incomplete, or form part of a continuing programme; this should be borne in mind when using or quoting from these documents.

Contract Reports are produced to record the results of scientific work carried out for sponsors, under contract. The ISVR treats these reports as confidential to sponsors and does not make them available for general circulation. Individual sponsors may, however, authorize subsequent release of the material.

UNIVERSITY OF SOUTHAMPTON

INSTITUTE OF SOUND AND VIBRATION RESEARCH

FLUID DYNAMICS AND ACOUSTICS GROUP

Stability and Accuracy of Finite Element Methods for Flow Acoustics: I. One Dimensional Acoustic Propagation

by

G Gabard and R J Astley

ISVR Technical Report No. 301

September 2003

Authorized for issue by
Professor R J Astley, Group Chairman

Contents

List of Figures

ABSTRACT

The dispersion properties of finite element models for aeroacoustic propagation based on the convected scalar Helmholtz equation and on the Galbrun equation are examined. The current study focusses on the effect of the mean flow on the dispersion and amplitude errors present in the the discrete numerical solutions. A general two-dimensional dispersion analysis is presented for the discrete problem on a regular unbounded mesh, and results are presented for the particular case of one dimensional acoustic propagation in which the wave direction is aligned with the mean flow. The magnitude and sign of the mean flow is shown to have a significant effect on the accuracy of the numerical schemes. Quadratic Helmholtz elements in particular are shown to be much less effective for downstream—as opposed to upstream—propagation, even when the effect of wave shortening or elongation due to the mean flow is taken into account. These trends are also observed in solutions obtained for simple test problems on finite meshes. A similar analysis of two-dimensional propagation is presented in an accompanying report.

I. INTRODUCTION

The behaviour of linear waves can be described by their dispersion properties[14]. As a consequence, the stability and accuracy of numerical methods for wave propagation problems can be assessed by comparing the dispersion properties of the waves described by the numerical model with those of the physical model.

The Helmholtz equation, which describes acoustic waves in a quiescent medium, has received particular attention and several studies have been devoted to finite element methods. A central issue in these studies is the pollution error which is known to be the main numerical error in practical cases. The pollution error is directly related to the dispersion error (see next section) and it is not controlled by keeping the number of points per wavelength constant.

Harari considered several finite element formulations for the two-dimensional Helmholtz equation with square bi-linear elements[5]. The dispersion, anisotropy and spurious reflections at a mesh discontinuity were analysed and it was shown that the Galerkin least square method gives the best overall results.

Deraemaeker *et al.* also analysed the dispersion error for the standard Galerkin formulation with p-hierarchic square elements and linear triangular elements[3]. The generalized-least-square, quasi-stabilized and residual-free-bubble methods were also compared.

The discontinuous Galerkin method was considered by Hu *et al.* for the wave equation in two dimensions[6]. The dispersion properties of this method proved to be mainly influenced by the expression of the numerical flux.

Mulder reported a systematic analysis of the dispersion properties of various finite element models for the one-dimensional Helmholtz equation[8]. He considered Lagrange, Gauss-Lobatto and Chebyshev elements, with order 1 to 5, and also without and with mass lumping. He showed that, for higher-order elements, the amplitude error should also be taken into account. This error can increase significantly for certain numbers of points per wavelength.

The dispersion analysis has also been used to assess the accuracy of other finite element methods such as the mesh-less Galerkin method[11] and a residual-based method[9].

The more general problem of acoustic wave propagation on a mean flow is of growing interest for engineering applications. However, very seldom work has been devoted to the dispersion properties of finite element methods for aeroacoustics. Astley *et al.* considered the one-dimensional linearized Euler equations solved with quadratic Lagrange and cubic Hermite elements[1]. The Galerkin method was shown to produce spurious numerical modes and the least square method achieves only a poor accuracy.

The present report is intended to study the dispersion properties of two finite element methods for solving aeroacoustic propagation problems. These numerical methods are based on the full potential theory and the Galbrun equation, respectively. In the first part of this report, we consider one-dimensional propagation along the mesh axes. The next section describes the dispersion analysis for finite element methods. In section III, the two numerical models for aeroacoustic propagation are presented. The dispersion properties of these methods are detailed in section IV. Finally, these results are compared with those of a simple test problem in section V.

The second part presents results for the two-dimensional acoustic propagation and especially the anisotropy of the dispersion properties of the numerical methods.

II. DISPERSION ANALYSIS

In this section, we describe the general framework to analyse dispersion properties of two-dimensional finite element methods for time-independent problems (e.g. steady or time-harmonic) with uniform coefficients. This framework can be easily modified for one- or three-dimensional problems.

Consider an infinite, two-dimensional, periodic mesh. Periodic means that the mesh is composed of a single 'pattern' of elements which is repeated in all directions to build the infinite mesh (two examples of mesh patterns are given in figure 3).

For this kind of mesh, it is possible to identify a finite number N of 'types' of nodes. All nodes of a given type share the same number of degrees of freedom and are located at the same place in the mesh pattern. Thus, all the nodes of given type form a regular grid and the position of a node of type p can be denoted by $\boldsymbol{x}_{m,n}^{(p)}$ where (m,n) are the indices of the node on the grid p. The node spacing is the same for all grids and is denoted δx and δy for the two directions. But most important, the equations corresponding to the degrees of freedom of a node of a given type are all identical. Hence, the global linear system is made up of N different sets of equations. For each type of node q,th e set of equations associated to the degrees of freedom is written:

$$\sum_{p=1}^{N}\sum_{m,n} A_{m,n}^{(q,p)} u_{m,n}^{(p)} = 0 \quad , \quad q = 1,2,\ldots,N \quad . \tag{1}$$

The vector $\boldsymbol{u}_{m,n}^{(p)}$ represents the M_p degrees of freedom of the node (m,n) of type p. The $M_q \times M_p$ matrix $\boldsymbol{A}_{m,n}^{(q,p)}$ describes the contributions of the node (m,n) of type p to the equations for a node of type q. These matrices obviously depend on the numerical method but also on all the problem parameters. The values of the indices (m,n) in the second sum depend on the node type q. It is also worth noting that in (1), the equations for a node of type q may involve degrees of freedom from other types of nodes.

From the sets of difference equations defined by (1) it is possible to obtain the dispersion relation of the numerical method. To that end, the general solution of the difference equations is written

$$u(\boldsymbol{x}_{m,n}^{(p)}) = u_0^{(p)} \alpha^m \beta^n \quad , \quad p = 1,2,\ldots,N \ , \tag{2}$$

where α and β are complex numbers. Since we consider an infinite mesh, we will consider only the complex numbers that have a unity norm ($|\alpha| = |\beta| = 1$) so that the wave amplitude remains bounded. Hence, we can define a real wavenumber

$$\boldsymbol{k} = k_x \boldsymbol{e}_x + k_y \boldsymbol{e}_y = k\boldsymbol{e}_x \cos\theta + k\boldsymbol{e}_y \sin\theta \quad ,$$

where θ is the wave propagation angle such that $\alpha = \exp(ik_x\delta_x)$ and $\beta = \exp(ik_y\delta_y)$. The expression (2) becomes

$$u(\boldsymbol{x}_{m,n}^{(p)}) = u_0^{(p)} \exp\left(i\boldsymbol{k}\cdot\boldsymbol{x}_{m,n}^{(p)}\right) \qquad p = 1,2,\ldots,N \ . \tag{3}$$

This is equivalent to using a Fourier transform to recast the equations (3) in the wavenumber domain. It is also useful to define $\kappa = \exp(ik)$, and, since we have a real wavenumber, κ is lying on the unity circle in the complex plane.

Each type of node has a different set of equations, so the degrees of freedom of a node of a given type have to be considered as independent of the degrees of freedom of other type of node. Thus, the wave amplitudes $\boldsymbol{u}_0^{(p)}$ are different for each type of node.

Substituting the plane wave solution (3) in the sets of equations (1) yields:

$$\sum_{p=1}^{N}\sum_{m,n} \boldsymbol{A}_{m,n}^{(q,p)} \boldsymbol{u}_0^{(p)} \alpha^m \beta^n = \boldsymbol{0}$$

$$\iff \sum_{p=1}^{N} \boldsymbol{F}^{(q,p)}(\alpha,\beta)\boldsymbol{u}_0^{(p)} = \boldsymbol{0} \ . \tag{4}$$

All the equations for $q = 1,2,\ldots,N$ can be expressed as a linear system for the wave amplitudes:

$$\begin{bmatrix} \boldsymbol{F}^{(1,1)} & \boldsymbol{F}^{(1,2)} & \cdots & \boldsymbol{F}^{(1,N)} \\ \boldsymbol{F}^{(2,1)} & \boldsymbol{F}^{(2,2)} & \cdots & \boldsymbol{F}^{(2,N)} \\ \vdots & \vdots & \ddots & \vdots \\ \boldsymbol{F}^{(N,1)} & \boldsymbol{F}^{(N,2)} & \cdots & \boldsymbol{F}^{(N,N)} \end{bmatrix} \begin{pmatrix} \boldsymbol{u}_0^{(1)} \\ \boldsymbol{u}_0^{(2)} \\ \vdots \\ \boldsymbol{u}_0^{(N)} \end{pmatrix} = \begin{pmatrix} \boldsymbol{0} \\ \boldsymbol{0} \\ \vdots \\ \boldsymbol{0} \end{pmatrix} \ . \tag{5}$$

This system, which can simply be written $\boldsymbol{RU} = \boldsymbol{0}$, is the numerical dispersion relation of the finite element model and represents an eigenvalue problem for k and $\boldsymbol{U}$, the other parameters being given.

To find non trivial solutions to the dispersion relation (5), the dispersion matrix $\boldsymbol{R}$ must be singular. Therefore, we have to solve the characteristic equation

$$\det(\boldsymbol{R}) = 0 \ , \tag{6}$$

for α and β, or equivalently for κ with a given value of θ. For each root $\bar{\kappa}$, we have $\tilde{k} = -i\ln(\bar{\kappa}) + 2n\pi$. So there is an infinite number of wavenumber solutions. Obviously, we only consider the case $n = 0$. Furthermore, each root $\tilde{k}$ of equation (6) is associated with an eigenvector $\tilde{\boldsymbol{U}}$ which is the right null vector of the matrix $\boldsymbol{R}$.

Of particular importance when solving equation (6) is the number of real roots k. The determinant $\det(\boldsymbol{R})$ is a polynomial in k whose order is defined by the functions $F^{(\cdot,\cdot)}$. The number of roots k in $\mathbb{C}$ is the order of the polynomial but the number of real roots depends on the parameters of the problem and cannot be known a priori.

Then, one has to match each solution $(\tilde{k}, \tilde{\boldsymbol{U}})$ of the numerical dispersion relation with an exact mode $(k, \boldsymbol{U})$ of the physical problem. If this is not possible, this mode is a spurious, or parasite, mode and the stability and convergence of the numerical method cannot be guaranteed.

With this dispersion analysis, the accuracy of the numerical model can be evaluated by defining two kind of errors. First, the well-known dispersion error is the deviation of the numerical wavenumber $\tilde{k}$ from its exact value k. In this report, we consider the relative dispersion error

$$e_d = \frac{\tilde{k}h - kh}{kh} \ , \quad E_d = |e_d| \ ,$$

where h is the finite element typical size. According to a result by Ihlenburg and Babuška[7], this error varies like

$$E_d \sim C\,(kh)^{2p} \ ,$$

where p is the order of the element and C is a constant independent of k and h.

The amplitude error is the deviation of $\tilde{\boldsymbol{U}}$ from its theoretical value $\boldsymbol{U}$ and is defined by

$$E_a = \frac{\left\|\tilde{\boldsymbol{U}} - \boldsymbol{U}\right\|}{\|\boldsymbol{U}\|} \ .$$

The numerical and exact eigenvectors are defined apart from a complex constant. To calculate a meaningful error E_a, it is necessary to choose a reference component in the eigenvector. The numerical and exact eigenvectors are normalized so that this reference component is 1.

It is worth noting that the amplitude error E_a is a local error whereas the dispersion error E_d is non local since it tends to accumulate as the wave propagates.

III. FINITE ELEMENT METHODS

In this section, we describe two finite element methods used to describe acoustic wave propagation in mean flows. These two methods are presented for time-harmonic problems, with a implicit time dependence given by $\exp(-i\omega t)$.

As explained in the previous section, all the parameters of the problem must be uniform in order to use the dispersion analysis. So we consider an homogeneous fluid (with density ρ_0 and speed of sound c_0) in uniform mean flow $\boldsymbol{v}_0$

$$\boldsymbol{v}_0 = Mc_0\cos(\alpha)\boldsymbol{e}_x + Mc_0\sin(\alpha)\boldsymbol{e}_y \ ,$$

where M is the Mach number and α is the mean flow direction.

III.1. Convected wave equation

A widespread model for acoustic waves in flows is the full potential theory with which the acoustic waves are described by means of the acoustic velocity potential. With this theory, the mean flow is irrotational. In the case of a uniform mean flow, this model reduces to the classical convected wave equation for the acoustic pressure:

$$\frac{\mathrm{d}_0^2 p}{\mathrm{d}t^2} - c_0^2\Delta p = 0 \ , \tag{7}$$

where $\mathrm{d}_0/\mathrm{d}t = -i\omega + \boldsymbol{v}_0\cdot\nabla$ is the material derivative in the mean flow. This equation can be expressed as the following variational statement for a domain Ω with boundary Γ:

$$\int_\Omega c_0^2\left(\nabla p\cdot\nabla\overline{p^\star}\right) - \frac{\mathrm{d}_0 p}{\mathrm{d}t}\frac{\overline{\mathrm{d}_0 p^\star}}{\mathrm{d}t}\mathrm{d}\Omega + \int_\Gamma \overline{p^\star}(\boldsymbol{v}_0\cdot\boldsymbol{n})\frac{\mathrm{d}_0 p}{\mathrm{d}t} - c_0^2\overline{p^\star}\boldsymbol{n}\cdot\nabla p\mathrm{d}\Gamma = 0 \ , \quad \forall p^\star \ , \tag{8}$$

where $p^\star$ is the pressure trial function and the overbar denotes the complex conjugate. This model is solved with various finite elements, see figure 1. The one-dimensional elements are the 2 node linear element (L2) and the 3 node quadratic element (L3). The two-dimensional elements comprise the 4 node bi-linear element (Q4), the 8 node 'serendipity' element (Q8) and the 9 node bi-quadratic element (Q9).

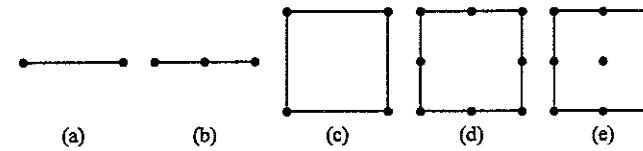

Figure 1 The finite elements for the convected wave equation: (a) 2 nodes linear element L2, (b) 3 nodes quadratic element L3, (c) 4 nodes bilinear element Q4, (d) 8 nodes serendipity element Q8 and (e) 9 nodes bi-quadratic element Q9.

III.2. Galbrun equation

The other model considered here is the Galbrun equation which is based on Lagrangian perturbation methods and is expressed for $\boldsymbol{w}$, the Lagrangian perturbation of the displacement[4]. This equation is valid for any type of mean flow and takes refraction effects by mean flow shear into account.

For an uniform mean flow, this equation reads

$$\rho_0\frac{\mathrm{d}_0^2\boldsymbol{w}}{\mathrm{d}t^2} - \rho_0 c_0^2\nabla\left(\nabla\cdot\boldsymbol{w}\right) = \boldsymbol{f} \ .$$

In order to be solved with finite elements, the Galbrun equation is expressed as a variational statement:

$$\int_\Omega \rho_0 c_0^2\left(\nabla\cdot\boldsymbol{w}\right)\left(\nabla\cdot\overline{\boldsymbol{w}^\star}\right) - \rho_0\frac{\mathrm{d}_0\boldsymbol{w}}{\mathrm{d}t}\cdot\frac{\overline{\mathrm{d}_0\boldsymbol{w}^\star}}{\mathrm{d}t}\mathrm{d}\Omega + \int_\Gamma \rho_0\left(\boldsymbol{v}_0\cdot\boldsymbol{n}\right)\frac{\mathrm{d}_0\boldsymbol{w}}{\mathrm{d}t}\cdot\overline{\boldsymbol{w}^\star} - \rho_0 c_0^2\left(\nabla\cdot\boldsymbol{w}\right)\overline{\boldsymbol{w}^\star}\cdot\boldsymbol{n}\mathrm{d}\Gamma = \int_\Omega \overline{\boldsymbol{w}^\star}\cdot\boldsymbol{f}\mathrm{d}\Omega \ , \quad \forall\boldsymbol{w}^\star \ , \tag{9}$$

where $\boldsymbol{w}^\star$ is the displacement trial function. With this variational formulation, originally proposed by Peyret and Élias[10],th e boundary integral is the momentum flux through the boundary[2] and the volume integral yields hermitian linear systems. This formulation is solved with the standard linear triangular element, see figure 2.

However, this displacement formulation is known to be unstable because spurious numerical modes are present. To circumvent this difficulty one can use a mixed formulation of Galbrun equation together with finite elements satisfying an inf-sup condition[13]. This issue is investigated in section IV.3 by means of the dispersion analysis. The Galbrun equation, expressed as a mixed formulation with the pressure variable, is:

$$\rho_0\frac{\mathrm{d}_0^2\boldsymbol{w}}{\mathrm{d}t^2} + \nabla p = \boldsymbol{f} \ ,$$

$$p + \rho_0 c_0^2\nabla\cdot\boldsymbol{w} = q \ .$$

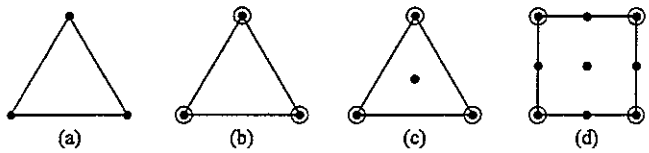

Figure 2 The finite elements for Galbrun's equation: (a) triangular linear element without pressure degree of freedom, (b) triangular linear element, (c) triangular linear element with a bubble function for the displacement and (d) square 9 nodes element with bilinear pressure and bi-quadratic displacement. (○ pressure node, • displacement node)

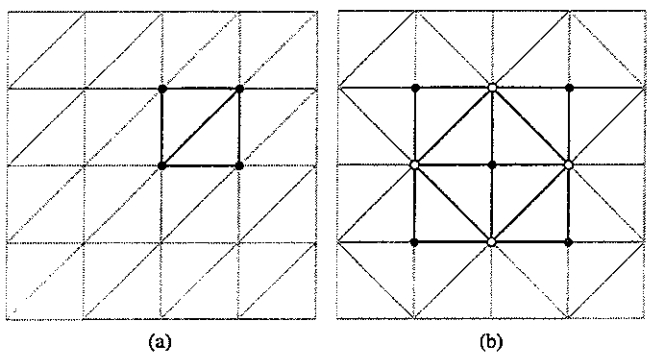

Figure 3 The two meshes used with the T4-3c Galbrun element: the mesh A (left) has one type of node, the mesh B (right) has two types of nodes (• and ○).

The corresponding variational statement is

$$\int_\Omega \overline{\boldsymbol{w}^\star}\cdot\nabla p + \boldsymbol{w}\cdot\nabla\overline{p^\star} - \rho_0\frac{\mathrm{d}_0\boldsymbol{w}}{\mathrm{d}t}\cdot\frac{\overline{\mathrm{d}_0\boldsymbol{w}^\star}}{\mathrm{d}t} - \frac{p\overline{p^\star}}{\rho_0 c_0^2}\mathrm{d}\Omega + \int_\Gamma \rho_0\left(\boldsymbol{v}_0\cdot\boldsymbol{n}\right)\frac{\mathrm{d}_0\boldsymbol{w}}{\mathrm{d}t}\cdot\overline{\boldsymbol{w}^\star} - \overline{p^\star}\boldsymbol{w}\cdot\boldsymbol{n}\mathrm{d}\Gamma = \int_\Omega \overline{\boldsymbol{w}^\star}\cdot\boldsymbol{f} - \frac{\overline{p^\star}q}{\rho_0 c_0^2}\mathrm{d}\Omega \quad , \quad \forall\left(\boldsymbol{w}^*, p^*\right) \quad , \quad (10)$$

where $p^\star$ is the pressure trial function. This formulation is solved with three different elements: the triangular linear element, the triangular linear element T4-3c with a 'bubble' function for the displacement and the 9 node square element Q9-4c with bi-quadratic displacement and linear pressure (see figure 2). Two different mesh patterns are considered for the T4-3c element, see figure 3.

III.3. Methodology

The two models which are considered here describe acoustic waves in moving fluid. With a uniform mean flow, the plane wave solutions can be written:

$$p = A\exp\left(i\boldsymbol{k}\cdot\boldsymbol{x} - i\omega t\right) \quad ,$$

$$\boldsymbol{w} = \frac{iA\boldsymbol{k}}{\rho_0\left(\omega - \boldsymbol{k}\cdot\boldsymbol{v}_0\right)^2}\exp\left(i\boldsymbol{k}\cdot\boldsymbol{x} - i\omega t\right) \quad ,$$

where A is the pressure wave amplitude and the wavenumber is given by

$$k = k\cos\theta\boldsymbol{e}_x + k\sin\theta\boldsymbol{e}_y \quad , \quad k = \frac{\omega}{c_0}\frac{1}{1 + M\cos\left(\theta - \alpha\right)} \quad . \quad (11)$$

In order to compare easily the efficiency of the various finite elements, the meshes used to compute the dispersion properties have the same node spacing which are denoted Δx and Δy. Thus, for a problem with a given size, the number of degrees of freedom can be considered as independent of the finite elements and their efficiencies can be readily compared. In this report, we only consider the case $\Delta x = \Delta y$.

To simplify the equations and the analysis, the density ρ_0 and the speed of sound c_0 are taken equal to 1 and the node spacing $h = \Delta x$ is constant while the other parameters are changed.

The accuracy of the finite element methods are analysed as functions of the free parameters M, α, θ and k. Since we choose the node spacing as the reference length scale, the wavenumber k is directly related to the number of points per wavelength. For given values of the free parameters, the theoretical pulsation ω is obtained with equation (11), the matrices $A_{m,n}^{(q,p)}$ are computed, the roots κ of the characteristic equation (6) are obtained with a Gauss-Newton iterative method (the `fsolve` function in Matlab) and finally the corresponding eigenvectors U are computed with a QR method (the `eig` function in Matlab).

To compute the amplitude error for Galbrun elements, the first pressure degree of freedom is used as the reference component.

IV. DISPERSION PROPERTIES

In this report, we study the accuracy of finite element methods for one dimensional propagation. That is, we consider only plane waves propagating along the e_x axis. Hence, $\alpha = \theta = 0$ and we have only two free parameters, namely the mean flow speed M and the wavenumber k. This simplification leads to a clear explanation of the important effects of the mean flow on the numerical accuracy. The effects of the direction of the wave with respect to the grid axes and to the mean flow direction will be discussed in a second report.

IV.1. Helmholtz linear elements

There is no spurious mode for the L2 and Q4 elements since their characteristic equations are of order 2. These two modes are the upstream and downstream acoustic waves.

The dispersion errors for the linear finite elements L2 and Q4 are identical and are given in figure 7. There is no amplitude error for these elements since their dispersion relation (5) is scalar. Clearly, the downstream and upstream propagation cases are different.

For upstream propagation, the mean flow tends to slightly increase E_d. The second-order convergence rate is well observed even for short waves (5 points per wavelength). It has to be noted that these effects are not produced by the wavelength shortening due to the Doppler effect since we consider E_d as a function of the number of points per wavelength.

For downstream propagation, the mean flow speed can significantly reduce the errors. For instance, with a 0.5 Mach number the dispersion error is divided by 2. Furthermore, for high mean flow speeds and short waves, E_d can be reduced to zero. This is more easily understood on figure 8 where E_d is plotted as a function of the Mach number. It is seen that the mean flow effect can balance the error of the numerical scheme and the error is then identically zero for some values of M and kh. Figure 8 also shows that the wavenumber is generally underestimated so the physical waves will lag behind the numerical ones. Finally, it is interesting to note that the effect of the mean flow can be modelled as roughly linear. In fact, the dispersion error on figure 8 is well approximated by $-C(1 - M)\left(kh\right)^2$.

IV.2. Helmholtz quadratic elements

Although it will not be detailled here, we have checked that, for $M \in (-1; 1)$ and with more than 4 points per wavelength (that is for all cases of practical interest), the quadratic elements L3, Q8 and Q9 have no spurious mode, i.e. modes which do not correspond to physical modes.

Figures 9 to 12 show the dispersion and amplitude errors for the elements L3, Q8 and Q9. The errors of this three elements are identical. This can be anticipated for the L3 and Q9 elements since shape functions for the latter are separable in each directions to obtain the L3 shape functions. But this is more surprising for the Q8 element.

For upstream propagation, the situation is similar to that of the linear elements, the fourth order convergence rate of E_d and E_a is well observed.

As for the linear elements, the mean flow effect is limited for the dispersion error but more pronounced for the amplitude error. This difference is much more evident for the downstream case. In that case, there is a difference of 2 orders of magnitude in E_a between the no flow case and $M = 0.9$. Furthermore, for downstream propagation and short waves, the errors can experience very important increases (as high as one order of magnitude). In the no flow case,

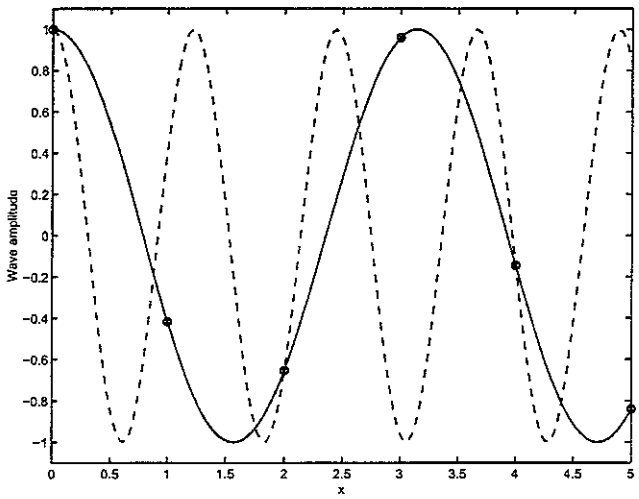

Figure 4 The physical wave and its copy for L3 elements. Solid line: a wave with wavenumber k; Dashed line: a wave with wavenumber $k+\pi$; o: nodal values for the mode with wavenumber k and eigenvector $(1,1)$; $\times$: nodal values for the mode with wavenumber $k+\pi$ and eigenvector $(1,-1)$.

this was noticed by Mulder[8] who referred to it as the aliasing error. For quadratic element, he considered it was not relevant to practical problems since it is found only for short waves (4 nodes per wavelength). But with mean flow the aliasing error may be present in practical situations (8-10 nodes per wavelength).

The aliasing error can be explained as follows. The L3 element dispersion relation possesses 4 real roots. Two correspond to the physical downstream k^+ and upstream k^- acoustic modes with eigenvectors equal to $(1,1)$. For the two other roots, the wavenumbers are $\tilde{k}^+ = k^+ + \pi/h$ and $\tilde{k}^- = k^- + \pi/h$ and the eigenvectors are $(1,-1)$. If we write the solution at the nodes for the mode $\tilde{k}^+$:

$$p(x_n) = \begin{cases} p_0^{(1)} \exp\left(in\tilde{k}^+ h\right) & , \text{ with } n \text{ even} , \\ p_0^{(2)} \exp\left(in\tilde{k}^+ h\right) & , \text{ with } n \text{ odd} , \end{cases}$$

$$= \begin{cases} \exp\left(ink^+ h + in\pi\right) = \exp\left(ink^+ h\right) & , \text{ with } n \text{ even} , \\ -\exp\left(ink^+ h + in\pi\right) = \exp\left(ink^+ h\right) & , \text{ with } n \text{ odd} , \end{cases}$$

it appears that the values at the node are the same as for the physical mode (it is also illustrated in figure 4). Thus, these two supplementary roots are not spurious modes since they also match the physical modes. However, when, for instance, the downstream mode k^+ and the copy of the upstream mode $\tilde{k}^-$ have the same wavenumber, the numerical model cannot describe properly these two modes with the same wavenumber but different eigenvectors. This results in an increase of the errors when $k^+ h = k^- h + \pi$. It is straightforward to see that it corresponds to

$$k^+ = \frac{\pi}{2h}(1-M) \quad .$$

With this simple equation it is possible to anticipate the peaks in dispersion and amplitude errors. As the mean flow speed increases, the aliasing error is presents for longer waves. However, the numerical wavenumbers corresponding to the peaks are underestimated by this equation since we used the exact expression (11) for the wavenumbers.

As for the linear elements, the dispersion error is found to vary almost linearly with the Mach number except for high speed flows where the aliasing error produces some kind of singularity in the curves (see figure 10). The dispersion error is well approximated by $-(1-M)(kh)^4$. On figure 12, it is also clear that the mean flow speed can have a very important effect on the amplitude error in the downstream propagation case. The amplitude error does not vary linearly with the Mach number.

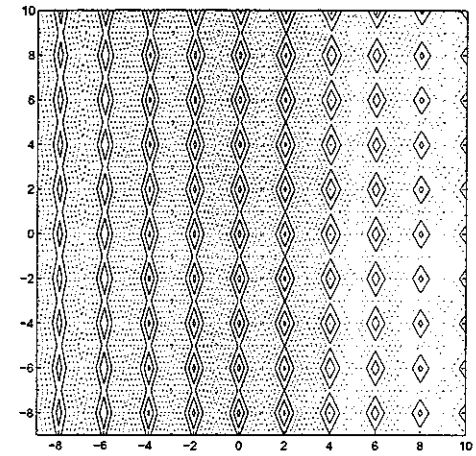

Figure 5 Pressure field for one of the spurious modes of the mixed formulation with the standard linear triangular finite element ($M=0$, $\omega=\pi/6$). 10 contours from -1 to 1, solid lines: positive values, dotted lines: negative values.

IV.3. Galbrun elements

A well-known problem when solving Galbrun equation with finite elements in the frequency domain is the occurrence of spurious numerical modes. This problem is also present without flow and, hence, is similar to that of displacement based acoustic formulations.

The problem is that the zero frequency rotational modes, which are exact solution of the problem, are described by the numerical model as non zero frequency modes. With standard finite elements, these modes will spoil the solution at any frequency.

Several authors have proposed specific numerical methods to cope with this problem. In this report, we use mixed finite elements satisfying the inf-sup condition proposed by Treyssède *et al.*[13]. It is worth investigating this issue by means of the dispersion analysis presented in this report.

First, we consider the displacement formulation defined by the variational statement (9) solved with the standard triangular linear element. The dispersion analysis shows that, apart the hydrodynamic mode and the two acoustic waves, this numerical model supports two other modes. It has been checked that these modes are purely rotational displacement fields and they are always present irrespective of the parameters ω and M.

Secondly, we consider the mixed triangular finite element without the bubble function (both p and w are linear). The dispersion analysis shows that this finite element, which does not satisfy the inf-sup condition, is not stable since there are 6 spurious modes. An example of the pressure field corresponding to one of these spurious modes is given in figure 5 and it is clearly a sawtooth pattern. These spurious modes are also present for all values of the parameters. This is consistent with a thorough study of Galbrun finite elements for duct acoustics[12]. This study shows that the mixed finite elements represent an improvement of the displacement based formulation. However, the stability of the mixed formulation with standard finite elements is not satisfying.

Similar spurious modes have already been reported for the one-dimensional linearized Euler equations solved with standard finite elements[1].

The occurrence of spurious modes with the Galbrun T4-3c element is found to depend on the Mach number. Spurious modes can exist if the mean flow Mach number is above 0.6 or below -0.6. The dispersion and amplitude errors for the T4-3c Galbrun finite element with the mesh A are given in figures 13 to 16. The behaviour of this element is quite different from the Helmholtz element.

In all cases the second order convergence rate is well observed both for E_d and E_a. The mean flow effect is more important for the dispersion error and in the case of upstream propagation. For instance, there is a difference of more than one order of magnitude in E_d between the no flow case and $M=0.9$. On the contrary,th e effect of the mean flow is very small for the amplitude error in the

downstream case.

It can be seen in figures 14 and 16 that the no flow case corresponds to a local maximum of the errors. However,E_d and E_a are significantly reduced when the Mach number increases and E_d is zero when $N \simeq -0.2$ and 0.25. This explains the important decreases of the dispersion error which can be seen in figure 13. It is also important to note that the errors can be quite large for upstream propagation and high speed mean flows.

The general trends observed with the mesh A are also obtained with the mesh B except for the occurrence of peaks for the amplitude error (see figures 17 to 20). These peaks are similar to those observed with the quadratic Helmholtz elements. This can be explained by noting that the mesh B has two different types of nodes (mesh A has only one type of node). Thus, if we have a root with wavenumber k and eigenvector $(p, w_x, w_y, p, w_x, w_y)$, we have another root with wavenumber $k + \pi/h$ and eigenvector $(p, w_x, w_y, -p, -w_x, -w_y)$. Furthermore, another difference with the mesh A is that the amplitude error is large for high speed mean flow both for upstream and downstream propagation.

These results show that the T43c Galbrun elements can give reliable results as long as the Mach number is not too high (less than 0.6). And, depending on the mesh pattern, the results may be altered by the aliasing error.

The errors for the 9 node Galbrun element with linear pressure are given in figures 21 to 24. Surprisingly, the convergence rate of the dispersion error is fourth order while for the amplitude it is only second order. This can be explained by the fact that the polynomial basis is not of the same order for the pressure and the dispacement. Furthermore, the effect of the mean flow is important for the dispersion error and the downstream propagation. In figures 22 and 24, it can be seen that the mean flow tends to reduce the dispersion and the amplitude errors. However, it is clear that the amplitude error remains very high (around 10%) compared to the triangular element T4-3c.

V. A TEST PROBLEM

It is important to evaluate to what extent the dispersion and amplitude errors influence the global numerical error for a practical problem. To that end, the results presented above are compared with the analysis of a simple test problem.

We consider the time-harmonic convected wave equation (7) on $[0, 2n\Delta x]$ with time dependence $\exp(-i\omega t)$. At $x = 0$ the pressure is set to 1 for the convected wave equation. For the Galbrun equation, at $x = 0$, the displacement is set so that the pressure is 1. At $x = 2n\Delta x$ the impedance condition $\partial p/\partial x = ikp$ is used with the theoretical value of the wavenumber given by (11). The exact solution to this problem is simply $p_{ex} = \exp(ikx)$. The domain is discretized by $2n$ linear elements or n quadratic elements so that the node spacing is always 1 and the number of degrees of freedom remains unchanged (see figure 6). For two-dimensional elements, the mesh is made of 4 (or 2) rows of linear (or quadratic) elements. In all cases, we use $n = 25$ and $\Delta x = 1$.

This simple problem is solved for various values of M and k, and for each case two numerical errors are defined:

$$E_1 = \frac{|p| - |p_{ex}|}{|p_{ex}|} \quad , \quad E_2 = \frac{|p - p_{ex}|}{|p_{ex}|} \quad .$$

These errors are computed at each node and we consider the mean values given in %. The first error is based on the pressure amplitude and is not influenced by the error on the phase. On the contrary, the second error takes into account the phase error. Thus, by comparing these two errors it is possible to identify the dispersion error from the other sources of error.

V.1. Helmholtz elements

Figures 25 and 26 give the numerical errors for the L2 element. The results for the Q4 element are strictly the same. The general behaviour of E_2 error is similar to the dispersion error (see figure 7): the mean flow only slightly increases the numerical error in the upstream propagation case and for the downstream case, the mean flow tends to reduce the error (especially for short wavelength). However for long waves it is unclear whether the mean flow is reducing or increasing the error because of oscillations. The E_1 error

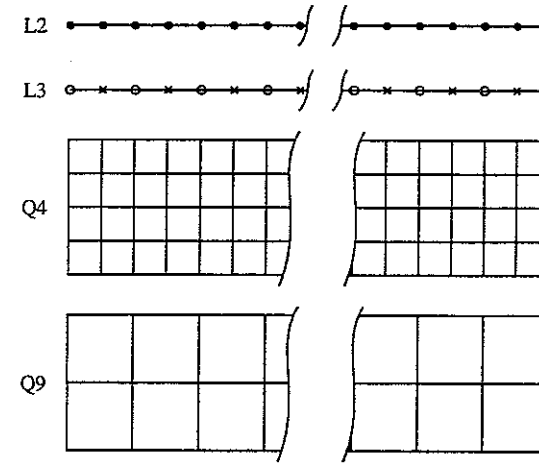

Figure 6 The one dimensional test problem with several kind of elements.

is very different: the convergence rate is only first order but the values are much smaller than E_2 (especially for short waves). The mean flow reduces (increases) E_2 in the upstream (downstream) case which is the contrary of the dispersion error for this element.

The numerical errors obtained with the L2 and Q9 elements are given in figures 27 and 28. Of particular importance is the fact that the peaks observed on E_1 and E_2 coincide with those of the dispersion and amplitude errors (see figures 9 and 11). This shows that the aliasing error can drive the numerical error even in practical cases (8-10 points per wavelength). Furthermore, the qualitative behaviour of E_1 and E_2 resemble the dispersion and amplitude errors. By comparing E_1 and E_2, one can notice that the mean flow effect is more pronounced for E_1. This is logical since E_1 does not take into account the phase error and hence is mainly influenced by the amplitude error (which varies significantly with the mean flow speed).

The fact that E_1an d $E_2$are very different with the linear elements and quite similar with the quadratic elements can be explained by the fact that the linear elements have no amplitude error. For the quadratic elements, E_2 is influenced by the dispersion and the amplitude errors whereas E_1 is only influenced by the amplitude error. With linear elements, $E_1$is not influenced by the amplitude error (these elements have no amplitude error) nor by the dispersion error (by definition of E_1), so it is likely that another source of error is observed with E_1 (probably the boundary conditions).

V.2. Galbrun elements

To use the T4-3c Galbrun element for the test problem, we use an alternating mesh similar to the mesh B given in figure 3. The results for the numerical errors E_1 and E_2 are given in figures 29 and 30.

The occurrence of spurious modes for high Mach number is clearly indicated by the peaks obtained for $M > 0.7$ and $M = -0.9$. For the other values of the Mach number,th e rate of convergence is not corresponding to the dispersion and amplitude error, so there is probably another source of error. Globally, it is found that the mean flow speed has an important effect on the numerical errors.

VI. CONCLUSIONS

For all the considered elements, the rates of convergence of the dispersion and amplitude errors are $2p$ regardless of the Mach number.

For the Helmholtz elements, we can conclude that:

(i) For the upstream propagation, the mean flow increases slightly the errors whereas, for the downstream propagation, the asymptotic errors can be significantly reduced by the mean flow.

(ii) For short waves and downstream propagation, the aliasing error can produce very important increases of the dispersion and amplitude errors.

(iii) The effect of the mean flow on the dispersion error is almost linear (except with the aliasing error).

(iv) The 8 and 9 node elements have the same dispersion properties.

Concerning the Galbrun elements:

(i) The effect of the mean flow is more important for upstream than for downstream propagation.

(ii) The stability is Mach number dependent: spurious modes may appear for $M > 0.6$ or $M < -0.6$.

(iii) The Q9-4c element is less efficient than the T4-3c. It can be explained by the fact that the pressure field is less precise with this element.

All these conclusions are also well observed with a simple test problem.

Mathematical analysis of finite element methods for the Helmholtz equation[7] provide asymptotic limits of the dispersion and numerical errors which are important to guarantee the robustness of these numerical methods. However, these results are not sufficient to describe the accuracy of finite element methods in the usual range of 8 to 15 points per wavelength. The results obtained with the quadratic Helmholtz elements (and especially the aliasing error) demonstrate that it is mandatory to assess finite element methods by means of the dispersion analysis in order to devise reliable rules for using these numerical models rather than relying on asymptotic error estimates.

REFERENCES

[1] R.J. Astley, N.J. Walkington, and W. Eversman. Accuracy and stability of finite element schemes for the duct transmission problem. *AIAA Journal*, 20:1547–1556, 1982.

[2] J.P. Brazier. Propagation acoustique au sein d'un écoulement non-uniforme. Technical report, ONERA, 23/3641 PY, 1996.

[3] A. Deraemaeker, I. Babuška, and P. Bouillard. Dispersion and pollution of the fem solution for the helmholtz equation in one, two and three dimensions. *International Journal for Numerical Methods in Engineering*, 46:471–499, 1999.

[4] H. Galbrun. *Propagation d'une onde sonore dans l'atmosphère terrestre et théorie des zones de silence*. Gauthier-Villars, 1931.

[5] I. Harari. Reducing spurious dispersion, anisotropy and reflection in finite element analysis of time-harmonic acoustics. *Computer Methods in Applied Mechanics and Engineering*, 140:39–58, 1997.

[6] F.Q. Hu, M.Y.Hussaini, and P. Rosetarinera. An analysis of the discontinuous galerkin method for wave propagation problems. *Journal of Computational Physics*, 151:921–946, 1999.

[7] F. Ihlenburg and I. Babuška. Finite element solution to the helmholtz equation with high wave number – part ii: the h-p-version of the fem. *SIAM Journal of Numerical Analysis*, 34(1):315–358, 1997.

[8] W.A. Mulder. Spurious modes in finite-element discretizations of the wave equation may not be all that bad. *Applied Numerical Mathematics*, 30:425–445, 1999.

[9] A.A. Oberai and P.M. Pinsky. A residual-based finite element method for the helmholtz equation. *International Journal for Numerical Methods in Engineering*, 49:399–419, 2000.

[10] C. Peyret and G. Élias. Finite-element method to study harmonic aeroacoustics problems. *Journal of the Acoustical Society of America*, 110(2):661–668, 2001.

[11] S. Suleau and P. Bouillard. One-dimensional dispersion analysis for the element-free galerkin method for the helmholtz equation. *International Journal for Numerical Methods in Engineering*, 47:1169–1188, 2000.

[12] F. Treyssède. *Etude de la propagation acoustique en présence d'écoulement non uniforme par une méthode d'éléments finis mixtes basée sur l'équation de Galbrun*. Thèse de doctorat, Université de Technologie de Compiègne, 2002.

[13] F. Treyssède, G. Gabard, and M. Ben Tahar. A mixed finite element method for acoustic wave propagation in moving fluids based on an eulerian-lagrangian description. *Journal of the Acoustical Society of America*, 113(2):705–716, 2003.

[14] G.B. Whitham. *Linear and nonlinear waves*. Wiley-Interscience, 1999.

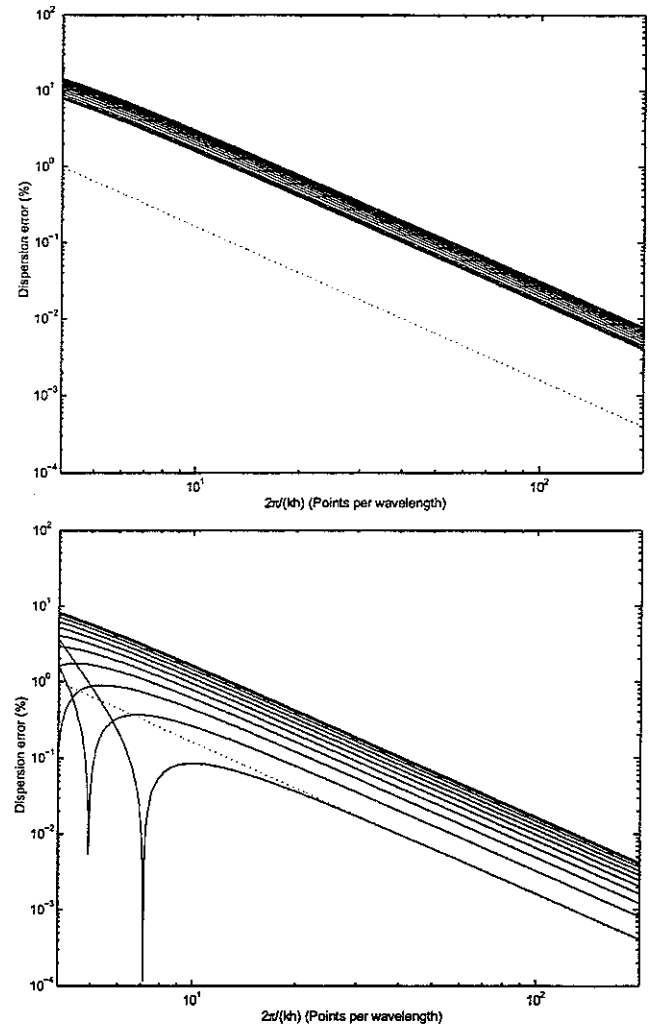

Figure 7 Dispersion error E_d (in %) for upstream (top) and downstream (bottom) propagation with the L2 and Q4 elements. Thick solid line: no flow case ($M = 0$); Solid lines: $M = \pm 0.1$ to ± 0.9 by an increment of 0.1. Dotted line: the second order slope.

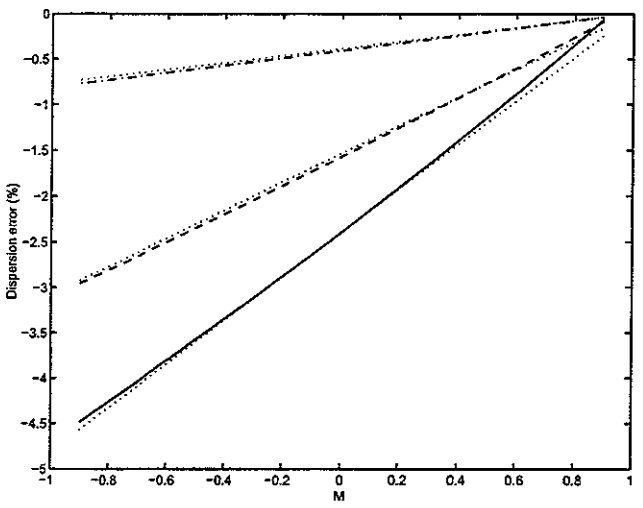

Figure 8 Dispersion error e_d (in %) as a function of the Mach number with the L2 and Q4 elements. Solid line: 8 points per wavelength; Dashed line: 10 points per wavelength; Dash-dotted line: 20 points per wavelength; Dotted lines: values obtained with $-(1 - M)(kh)^2$.

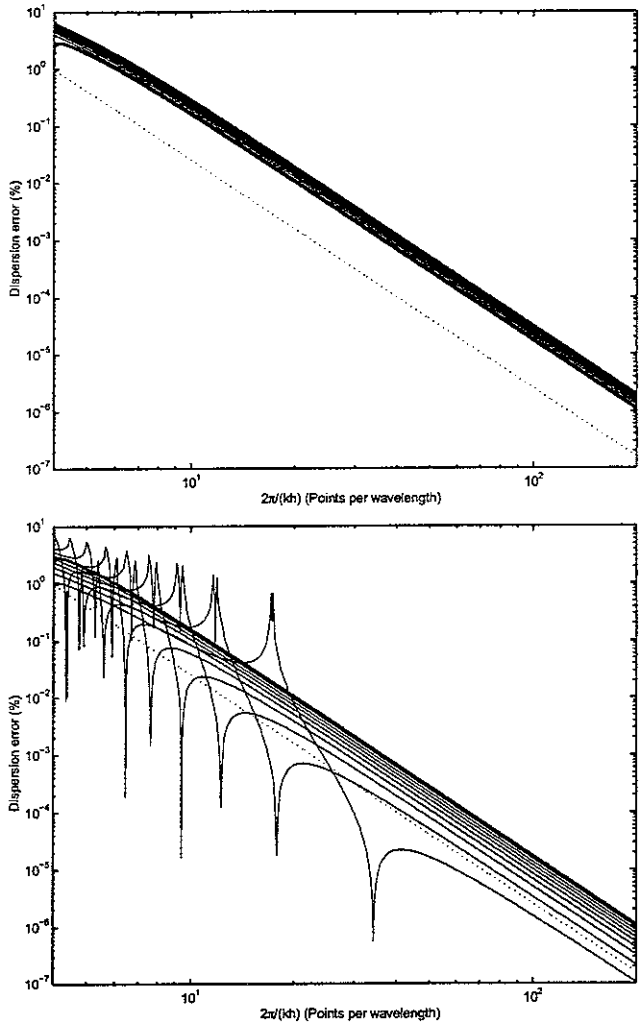

Figure 9 Dispersion error E_d (in %) for upstream (top) and downstream (bottom) propagation with the L3, Q8 and Q9 elements. Thick solid line: no flow case ($M = 0$); Solid lines: $M = \pm 0.1$ to ± 0.9 by an increment of 0.1. Dotted line: the fourth order slope.

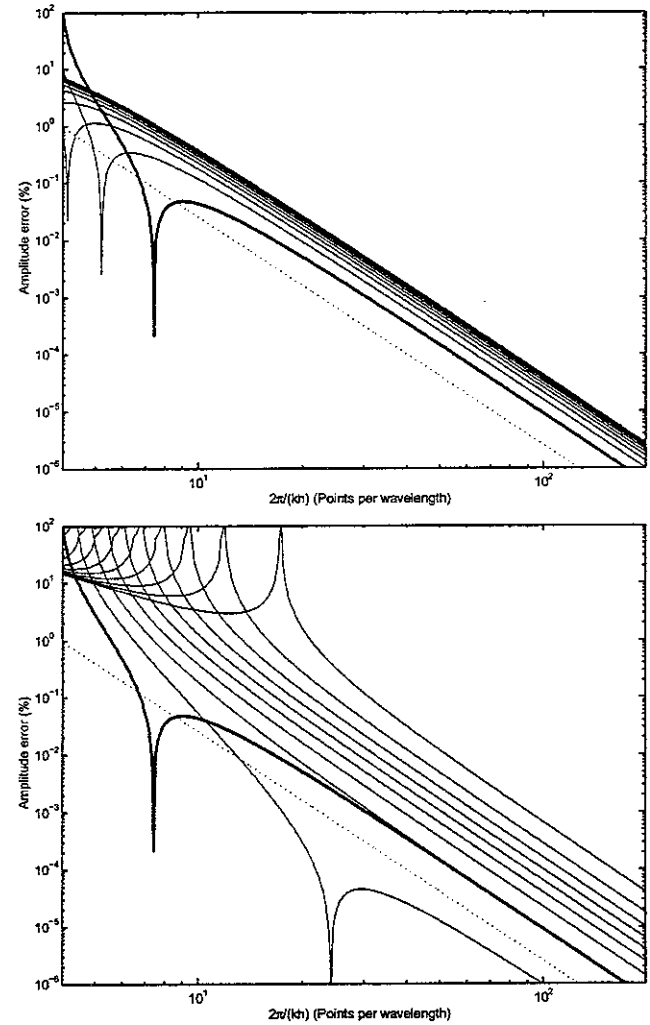

Figure 11 Amplitude error E_a (in %) for upstream (top) and downstream (bottom) propagation with the L3, Q8 and Q9 elements. Thick solid line: no flow case ($M = 0$); Solid lines: $M = \pm 0.1$ to ± 0.9 by an increment of 0.1. Dotted line: the fourth order slope.

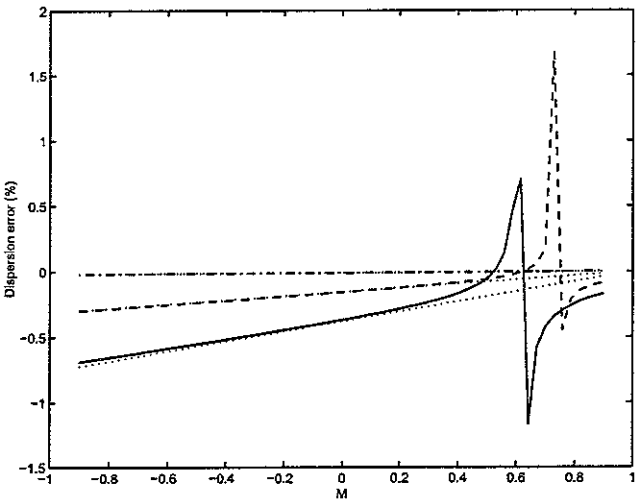

Figure 10 Dispersion error e_d (in %) as a function of the Mach number with the L3, Q8 and Q9 elements. Solid line: 8 points per wavelength; Dashed line: 10 points per wavelength; Dash-dotted line: 20 points per wavelength; Dotted lines: values obtained with $-(1-M)(kh)^4$.

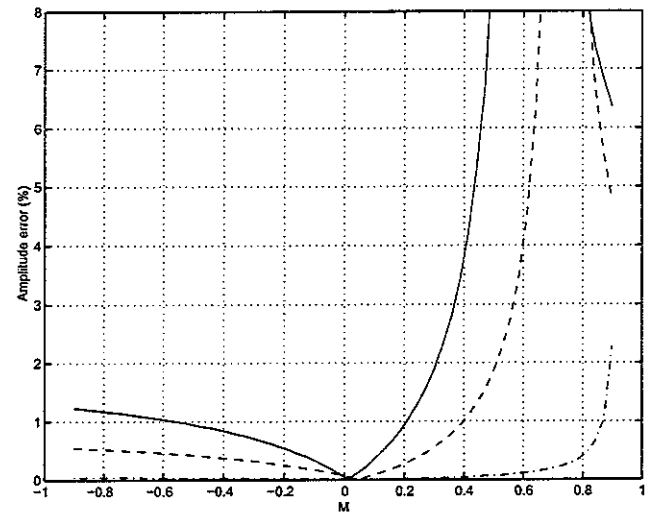

Figure12 Amplitude error E_a (in %) as a function of the Mach number with the L3, Q8 and Q9 elements. Solid line: 8 points per wavelength; Dashed line: 10 points per wavelengths; Dash-dotted line: 20 points per wavelength.

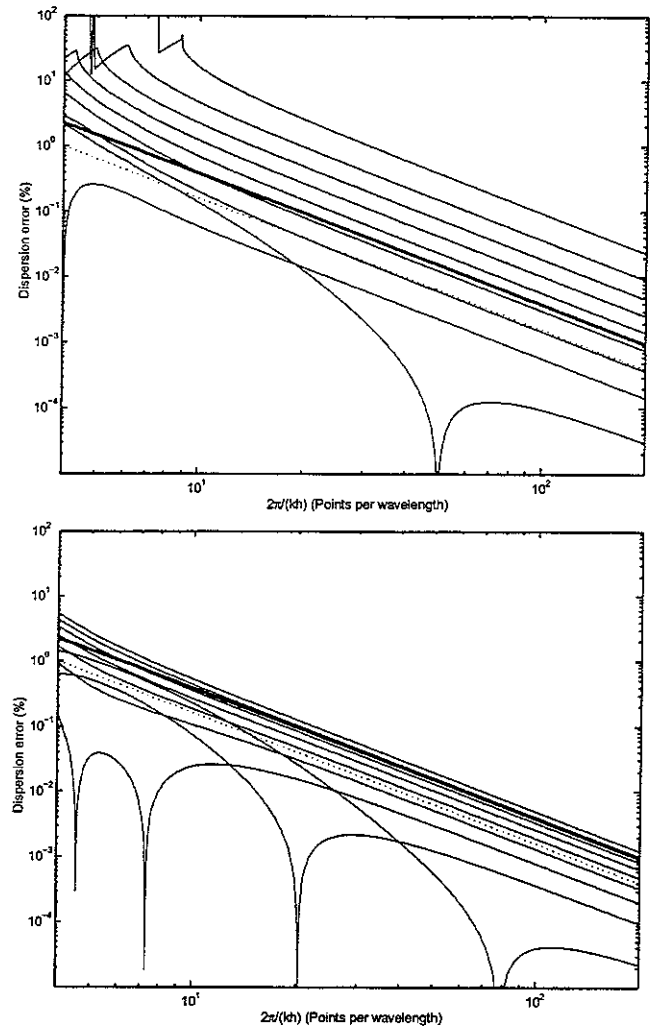

Figure 13 Dispersion error E_d (in %) for upstream (top) and downstream (bottom) propagation with the T4-3c Galbrun element with mesh A. Thick solid line: no flow case ($M = 0$); Solid lines: $M = \pm 0.1$ to ± 0.9 by an increment of 0.1. Dotted line: the second order slope.

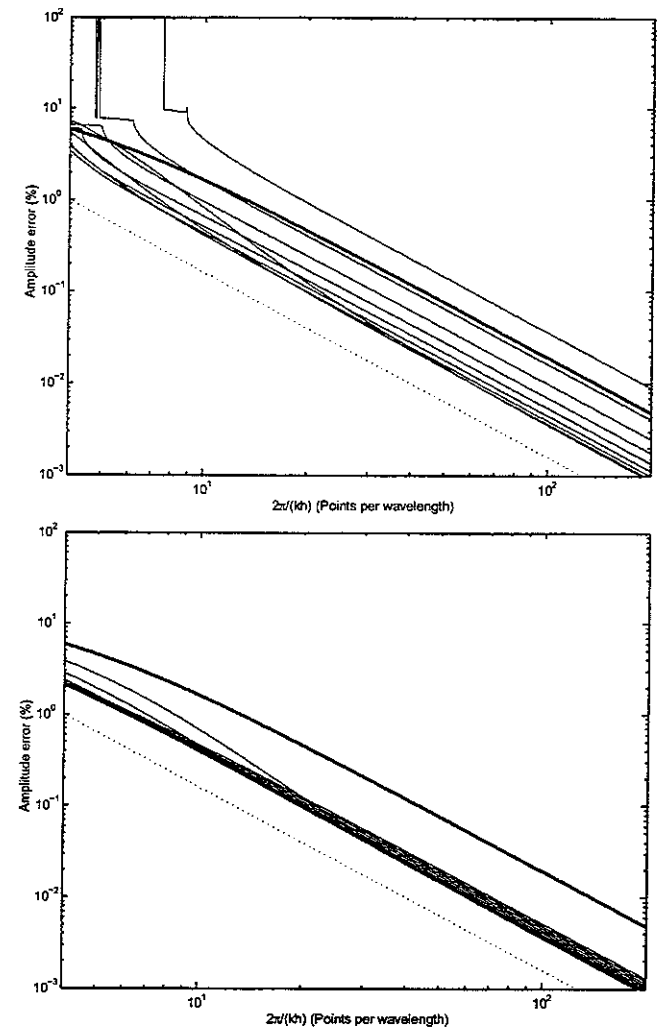

Figure 15 Amplitude error E_a (in %) for upstream (top) and downstream (bottom) propagation with the T4-3c Galbrun element with mesh A. Thick solid line: no flow case ($M = 0$); Solid lines: $M = \pm 0.1$ to ± 0.9 by an increment of 0.1. Dotted line: the second order slope.

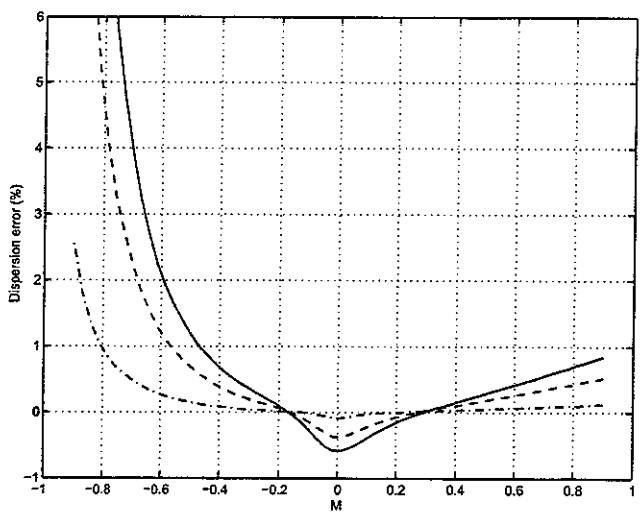

Figure 14 Dispersion error e_d (in %) as a function of the Mach number with the T4-3c Galbrun element with mesh A. Solid line: 8 points per wavelength; Dashed line: 10 points per wavelength; Dash-dotted line: 20 points per wavelength.

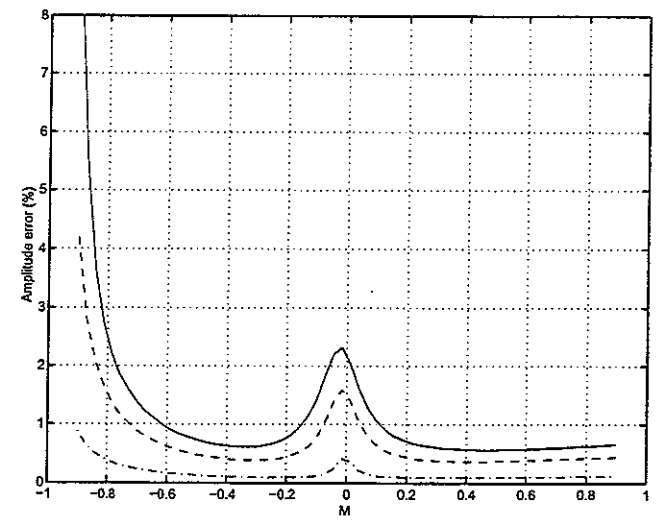

Figure 16 Amplitude error E_a (in %) as a function of the Mach number with the T4-3c Galbrun element with mesh A. Solid line: 8 points per wavelength; Dashed line: 10 points per wavelength; Dash-dotted line: 20 points per wavelength.

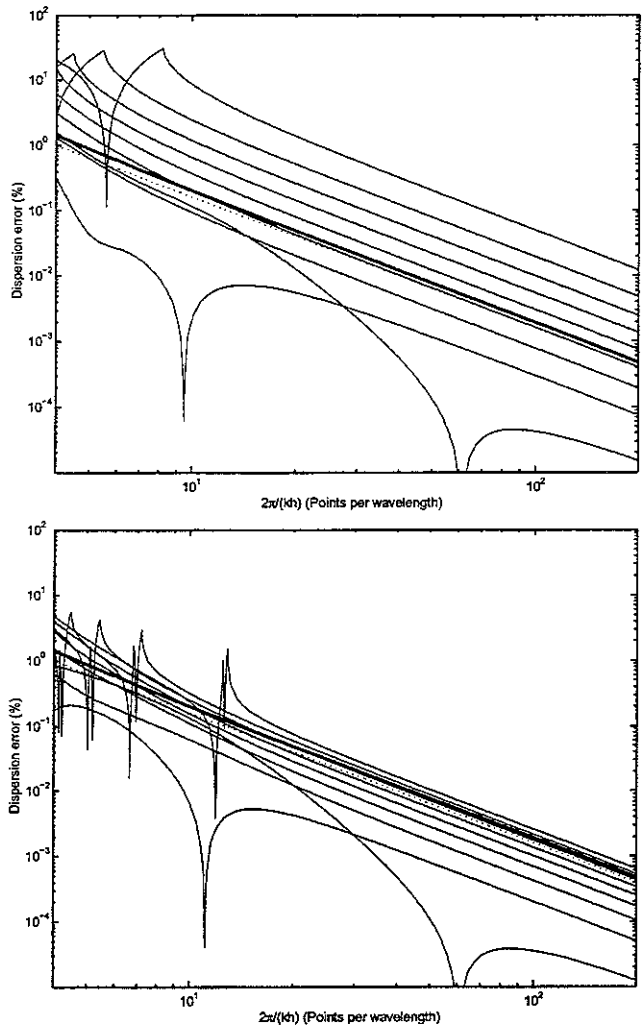

Figure 17 Dispersion error E_d (in %) for upstream (top) and downstream (bottom) propagation with the T4-3c Galbrun element with mesh B. Thick solid line: no flow case ($M = 0$); Solid lines: $M = \pm 0.1$ to ± 0.9 by an increment of 0.1. Dotted line: the second order slope.

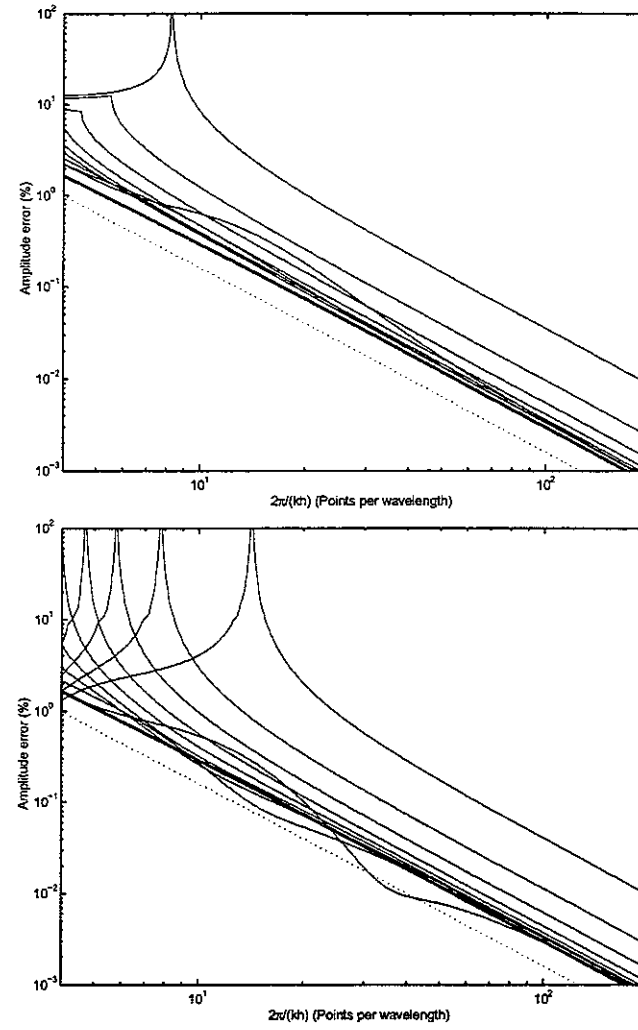

Figure 19 Amplitude error E_a (in %) for upstream (top) and downstream (bottom) propagation with the T4-3c Galbrun element with mesh B. Thick solid line: no flow case ($M = 0$); Solid lines: $M = \pm 0.1$ to ± 0.9 by an increment of 0.1. Dotted line: the second order slope.

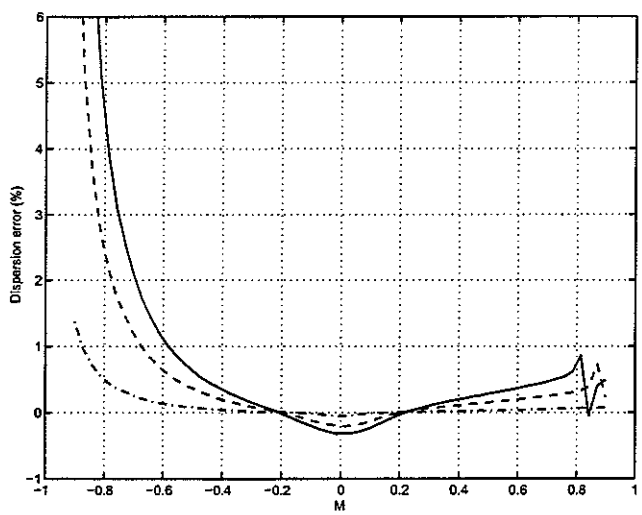

Figure 18 Dispersion error e_d (in %) as a function of the Mach number with the T4-3c Galbrun element with mesh B. Solid line: 8 points per wavelength; Dashed line: 10 points per wavelength; Dash-dotted line: 20 points per wavelength.

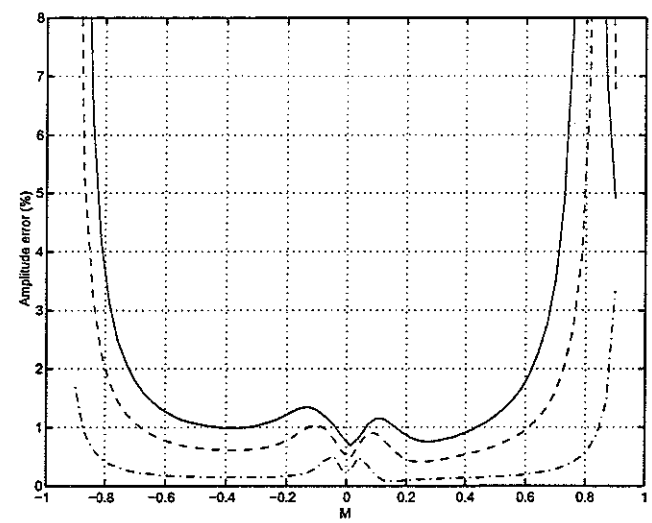

Figure 20 Amplitude error E_a (in %) as a function of the Mach number with the T4-3c Galbrun element with mesh B. Solid line: 8 points per wavelength; Dashed line: 10 points per wavelength; Dash-dotted line: 20 points per wavelength.

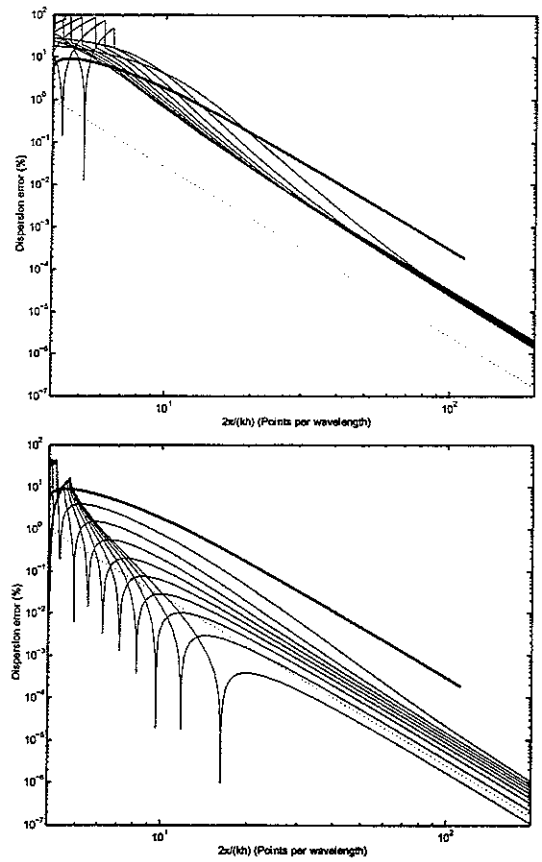

Figure 21 Dispersion error E_d (in %) for upstream (top) and downstream (bottom) propagation with the Q9-4c Galbrun element. Thick solid line: no flow case ($M = 0$); Solid lines: $M = \pm 0.1$ to ± 0.9 by an increment of 0.1. Dotted line: the second order slope.

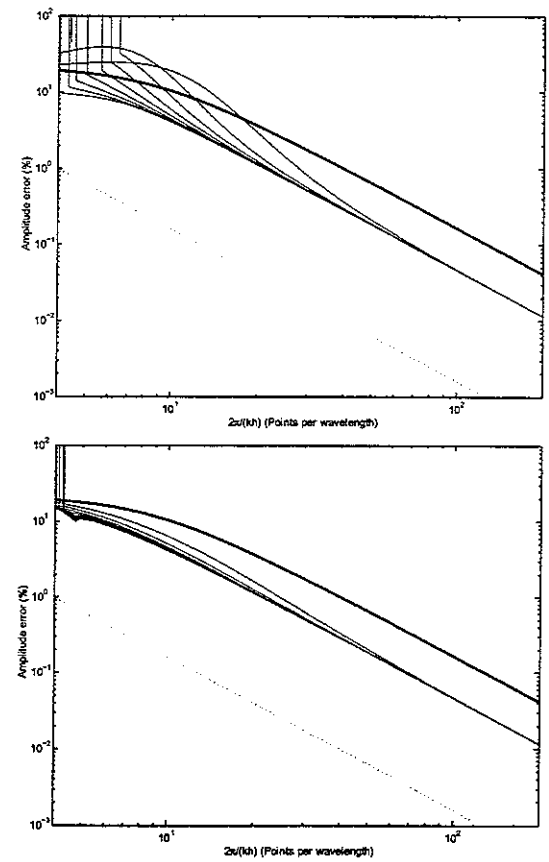

Figure 23 Amplitude error E_a (in %) for upstream (top) and downstream (bottom) propagation with the Q9-4c Galbrun element. Thick solid line: no flow case ($M = 0$); Solid lines: $M = \pm 0.1$ to ± 0.9 by an increment of 0.1. Dotted line: the second order slope.

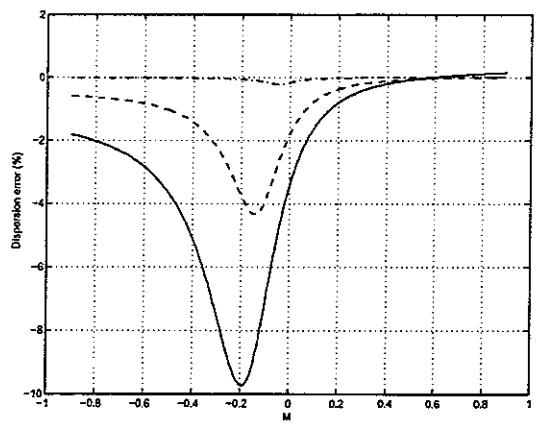

Figure 22 Dispersion error e_d (in %) as a function of the Mach number with the Q9-4c Galbrun element. Solid line: 8 points per wavelength; Dashed line: 10 points per wavelength; Dash-dotted line: 20 points per wavelength.

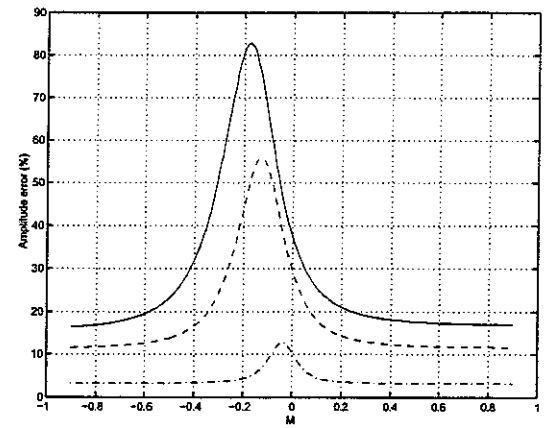

Figure24 Amplitude error E_a (in %) as a function of the Mach number with the Q9-4c Galbrun element. Solid line: 8 points per wavelength; Dashed line: 10 points per wavelength; Dash-dotted line: 20 points per wavelength.

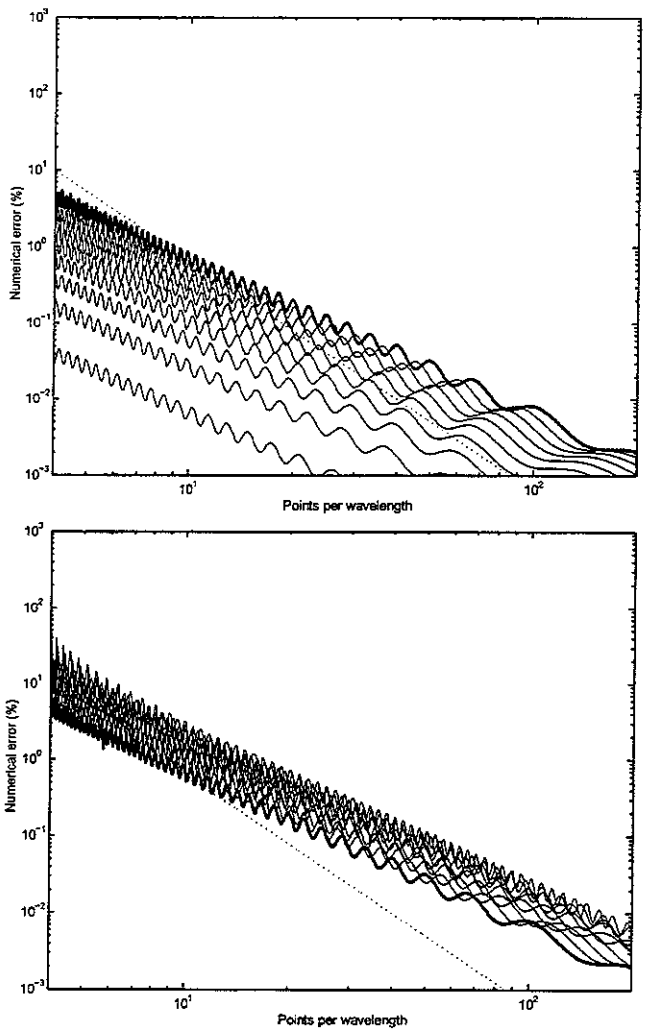

Figure 25 Averaged numerical error E_1 (in %) for upstream (top) and downstream (bottom) propagation with the L2 and Q4 elements. Thick solid line: no flow case ($M = 0$); Solid lines: $M = \pm 0.1$ to ± 0.9 by an increment of 0.1. Dotted line: the third order slope.

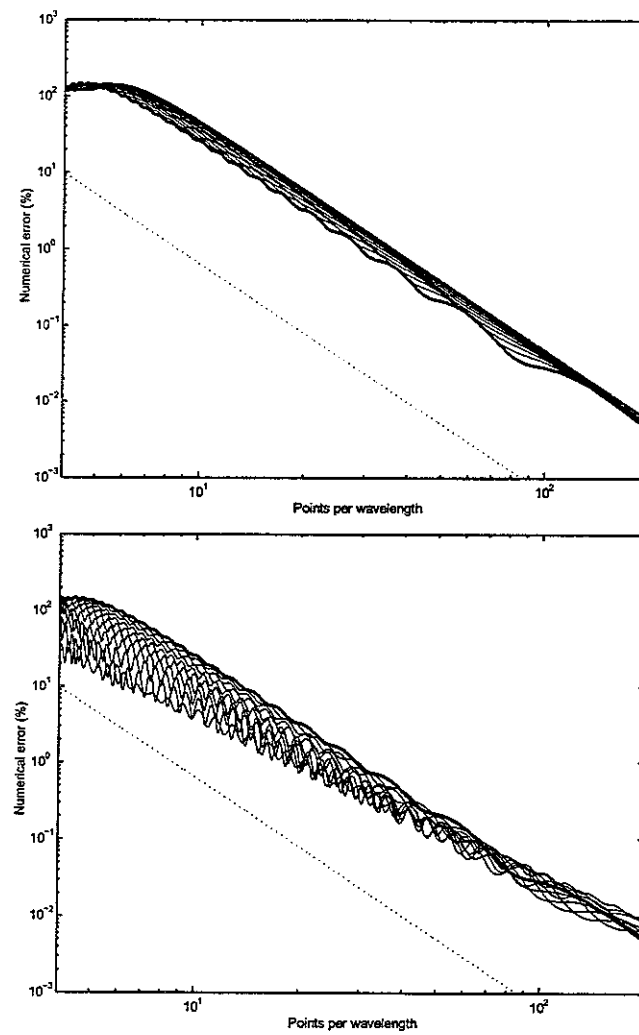

Figure 26 Averaged numerical error E_2 (in %) for upstream (top) and downstream (bottom) propagation with the L2 and Q4 elements. Thick solid line: no flow case ($M = 0$); Solid lines: $M = \pm 0.1$ to ± 0.9 by an increment of 0.1. Dotted line: the third order slope.

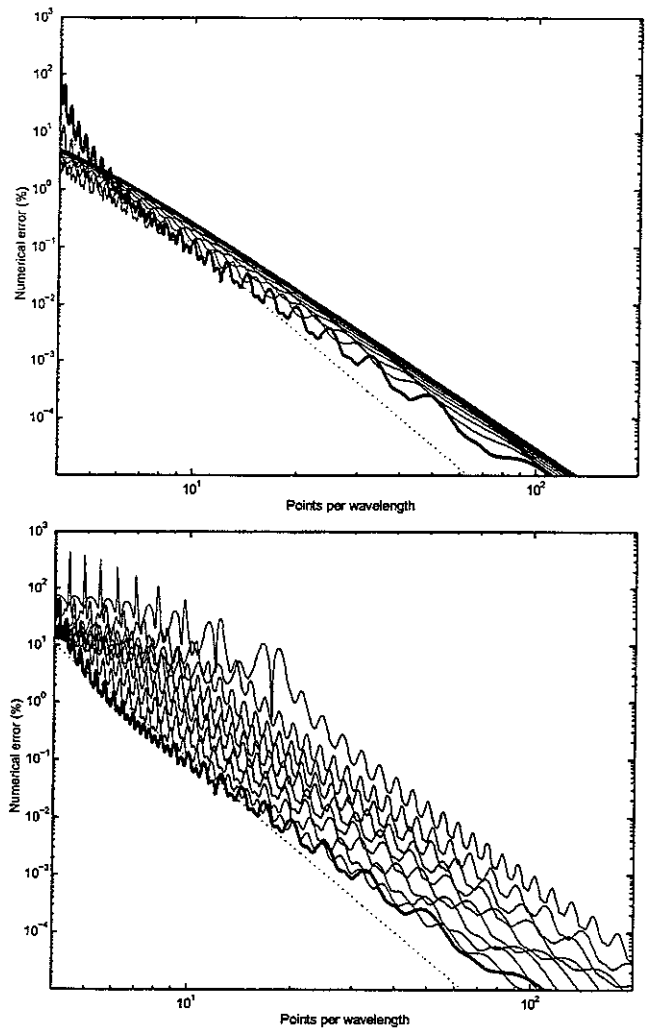

Figure 27 Averaged numerical error E_1 (in %) for upstream (top) and downstream (bottom) propagation with the L3 and Q9 elements. Thick solid line: no flow case ($M = 0$); Solid lines: $M = \pm 0.1$ to ± 0.9 by an increment of 0.1. Dotted line: the fifth order slope.

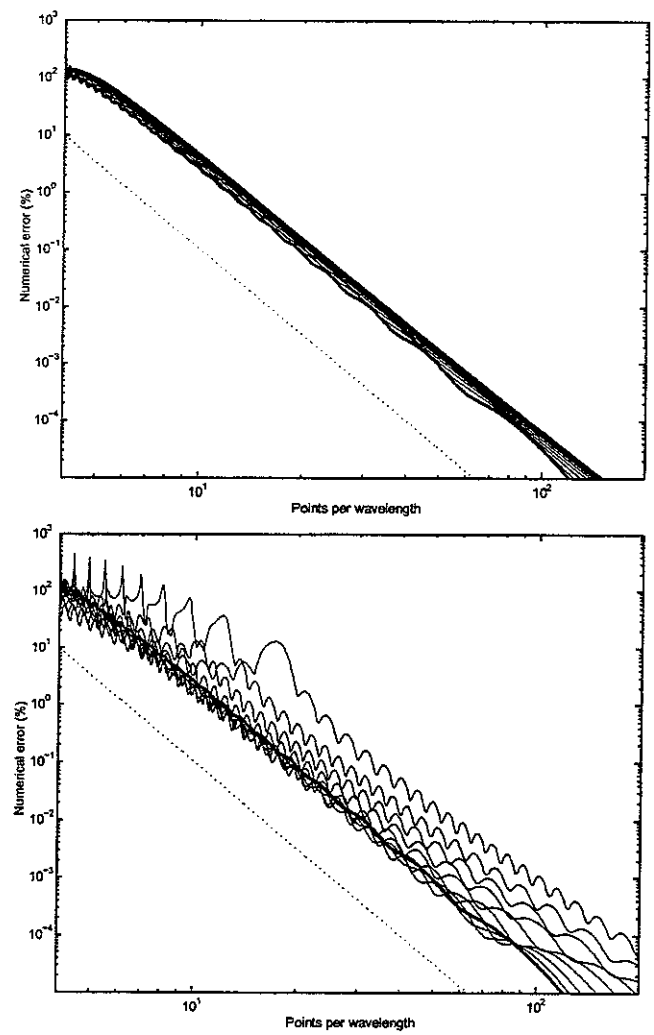

Figure 28 Averaged numerical error E_2 (in %) for upstream (top) and downstream (bottom) propagation with the L3 and Q9 elements. Thick solid line: no flow case ($M = 0$); Solid lines: $M = \pm 0.1$ to ± 0.9 by an increment of 0.1. Dotted line: the fifth order slope.

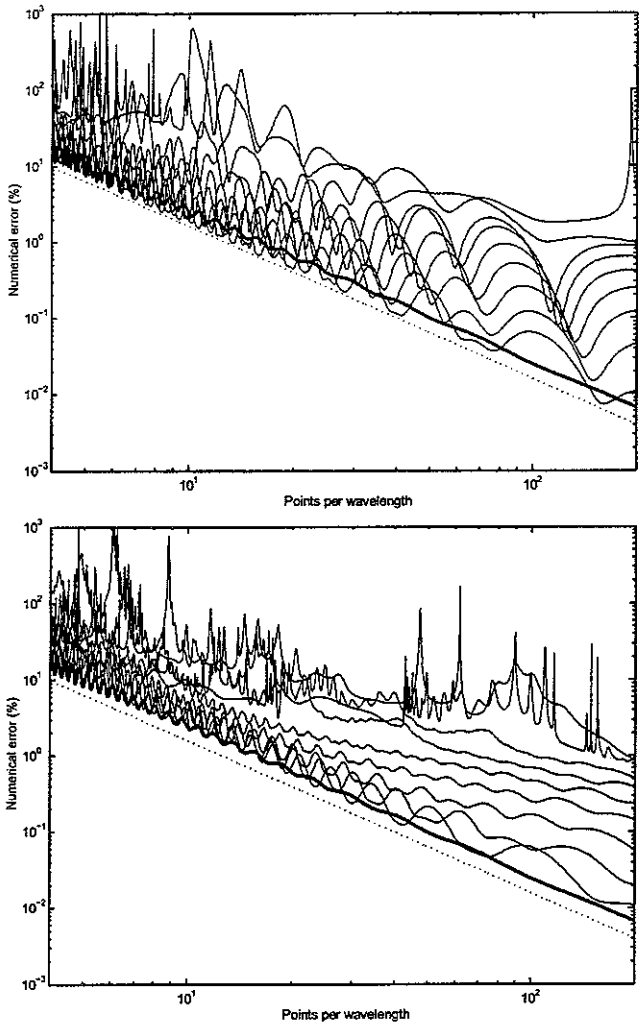

Figure 29 Averaged numerical error E_1 (in %) for upstream (top) and downstream (bottom) propagation with the Galbrun T4-3c element for the mesh B. Thick solid line: no flow case ($M = 0$); Solid lines: $M = \pm 0.1$ to ± 0.9 by an increment of 0.1. Dotted line: the second order slope.

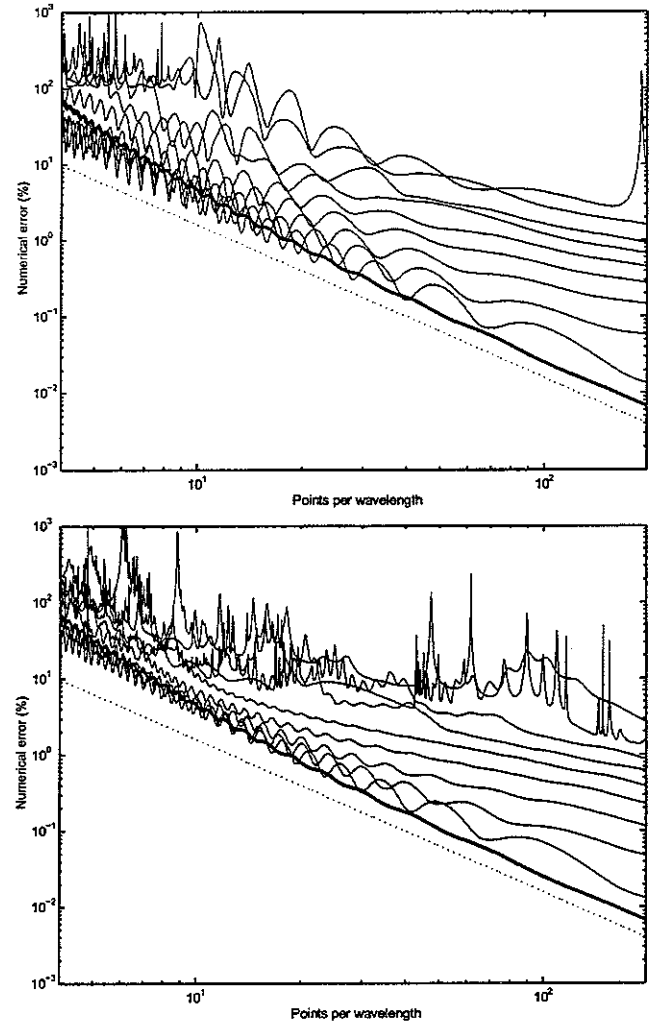

Figure 30 Averaged numerical error E_2 (in %) for upstream (top) and downstream (bottom) propagation with the Galbrun T4-3c element for the mesh B. Thick solid line: no flow case ($M = 0$); Solid lines: $M = \pm 0.1$ to ± 0.9 by an increment of 0.1. Dotted line: the second order slope.